Electronic Supplementary Material (ESI) for Soft Matter.

Supporting information

Kinetic state diagrams for a highly asymmetric block copolymer assembled in solution

M. Paula Vena [1,2], Demi de Moor [1,2], Alessandro Ianiro[1,3], Remco Tuinier[1,2], Joseph P. Patterson[4]*

[1]*Laboratory of Physical Chemistry, Department of Chemical Engineering and Chemistry, Eindhoven University of Technology, P.O. Box 513, 5600 MB, Eindhoven, The Netherlands*

[2]*Institute for Complex Molecular Systems, Eindhoven University of Technology, P.O. Box 513, 5600 MB, Eindhoven, The Netherlands*

[3]*Adolphe Merkle Institute, University of Fribourg, Chemin des Verdiers 4, CH-1700, Fribourg Switzerland*

[4]*Department of Chemistry, University of California - Irvine, 1102 Natural Sciences II, Irvine, California 92697, United States*

**Correspondence to: patters3@uci.edu*

MATERIALS AND METHODS

Materials

Reagents were purchased from commercial sources and used without further purification.

Characterization methods

^{1}H Nuclear Magnetic Resonance

The number-averaged molar mass M_n^{NMR} of the synthesized copolymers was calculated by ^{1}H NMR, carried out on a Varian 400 (400 MHz) spectrometer at 25 °C in deuterated chloroform.

The molar mass of the PS block was determined from the ratio between the integrals of the broad peak between 6.5 and 7.0 ppm, and the peak at 3.4 ppm. The first peak is associated with the 5 protons on the aromatic rings of the PS block while the second peak is associated with the 3 protons in the terminal CH_3 group of the PEO block. This gives a DP_{PS} = 250 and DP_{PEO} = 45.

Size exclusion chromatography

The molar mass dispersity $Đ = M_w/M_n$, were M_w is the weight-averaged molar mass, was determined from the molar mass distribution obtained by means of size exclusion chromatography (SEC), using a Waters GPC equipped with Waters (model 510) pump and a (model 410) differential refractometer. A set of two mixed bed columns (Mixed-C, Polymer Laboratories, 30 cm, 40 °C) was used and THF was selected as eluent. The system was calibrated using narrow molar mass polystyrene standards, ranging from 162 to 30230 Da.

Transmission Electron Microscopy

TEM images were acquired on a TFS Tecnai Sphera at 200 kV. Sample preparation was performed as follows: 10 µL of sample were deposited on a 200 copper mesh grid with continuous carbon support film that was previously glow discharged for 40 s with a Cressington 208 carbon coater to enhance the hydrophilicity of the support. After 45 s the excess of liquid was blotted away using a filter paper and

the grid left to dry out. ImageJ and an in-house Matlab script were used to measure particle size from TEM images. Sizes are based on averaging over 100 particles.

Cryo Transmission Electron Microscopy

CryoTEM was performed on selected assemblies to confirm that the drying effect are neglectable. Samples ere prepared on 200 mesh copper TEM grids with a hydrophilized R2/2 Quantifoil carbon support film (Quantifoil Micro Tools GmbH, Jena, Germany). Surface plasma treatment was used to hydrophilize the support film. 3 µL of sample were applied on the TEM grid, blotted and vitrified using a TFS Vitrobot™ Mark IV by plunging into liquid ethane. Cryo-TEM was performed on the TU/e cryoTITAN (TFS, www.cryotem.nl) operated at 300 kV, equipped with a field emission gun, a post column Gatan Energy Filter (GIF) and a post-GIF 2k × 2k Gatan CCD Camera.

Experimental

Synthesis of poly(ethylene oxide)-*b*-polystyrene

The synthesis of the PS_{250}-*b*-PEO_{45} polymer was done via a standard ATRP procedure with CuBr as catalyst: CuBr was purified by washing five times with glacial acetic acid, twice with absolute ethanol and twice with diethyl ether then added to a dried Schlenk flask equipped with a stir bar. After sealing with a rubber septum, the flask was degassed and backfilled with nitrogen (N_2) five times and then left under N_2. Subsequently, a mixture of styrene, PEO-methyl ether- 2-bromoisobutyrate (PEO-Me-BrIB), and N,N,N',N'',N''-pentadimethyldiethylenetriamine (PMDETA), was added to a glass vial under N_2, heated up to 120 °C and degassed by bubbling dry nitrogen in the melt for 1 h. The mixture was then transferred to the Schlenk flask containing the catalyst, which was placed in a thermostated oil bath at 120 °C for 24 h. The purification was performed by dissolving the product in dichloromethane followed by precipitation in hexane.

^{1}H NMR ($CDCl_3$, TMS, 400 MHz): δ = 1.43 ppm (br, PS aliphatic backbone), δ = 1.58 ppm (s, water), δ = 1.85 ppm (br, PS aliphatic backbone), δ = 3.38 ppm (s, 3H), δ = 3.64 ppm (t, 190.15H), δ = 6.45, 6.57, 7.03 ppm (br, 1248,81H), δ = 7.24 ppm (s, CDCl3) (Figure S1.c)

Preparation of aqueous dispersions of PS-*b*-PEO block copolymer *via* solvent switch

We explored the effect of polymer concentration, temperature and solvent addition rate in the self-assembly of PS_{250}-*b*-PEO_{45}. All other parameters that could affect the self-assembly process (i.e. vial size, stirring bar size, stirring rate, syringe and needle size) were fixed. A 10 mg/mL stock solution of the polymer in THF was prepared and all experiments were performed by taking aliquots of the stock solution to minimize weighing errors. Experiments were performed in the dilute regime, below the overlap concentration.[1]

In a typical procedure, an aliquot of the stock solution was diluted with THF to a final volume of 1 mL and the desired final concentration (0.1 mg/mL, 1 mg/mL and 10 mg/mL) in a 4 mL glass vial. The solution was equilibrated at the temperature of the experiment. Experiments at T = 20, 40 and 60 °C were performed in an oil bath while at T = 4 °C a cooling system was used.

1 mL of milli-Q water was added from a 10 mL syringe (BD plastic, diameter: 14.5 mm) to the polymer solution using a Harvard Apparatus 11 plus syringe pump to regulate the rate addition. Three different rate additions were used: 1 mL/min, 1 mL/h and 1 mL/d. The stirring rate was set to 500 rpm.

After the water addition was finished, dialysis was carried on for two days to remove the THF using 1 mL dialysis capsules (QuixSep) covered with a dialysis membrane (Spectra/Por R©7) with a cut-off at 3.5 kDa. The aqueous dispersions were stored for up to 1.5 years at room temperature (Figure S5).

Classification of assemblies

Classification criteria

The assemblies were classified based on their 2D projection images and line profiles (Figure S6). For some of the more complex structures Electron Tomography is often employed to fully resolve the 3D structure.[2, 3] The morphologies found here have been well studied previously,[4, 5] and therefore can be assigned from the 2D projection images with confidence. Here, we also choose to classify the structures based on their surface and internal structure. The surface can be classified into solid (S), broken (B) and porous (P). The internal structure as hollow (H), solid (S), with isolated pores (IP) and with connected pores (CP).

S(S): Large compound micelles[6]

Large compound micelles (LCM) with sizes ranging from 80 nm to 280 nm were found at an initial polymer concentration of 0.1 mg/mL. They are polydisperse large spheres composed of inverse micelles. They are thought to be related mechanistically to the so-called nano-bowls. [6]

S(H): Vesicles

Vesicles are found for almost all studied conditions at initial concentration of polymer of 10 mg/mL. In some cases, the vesicles are slightly collapsed, presenting a typical indentation pattern or an oblate shape, or highly collapsed like stomatocytes[7] or *kippa*[8] shape.

B(S), B(H), B(IP), B(CP): nano-bowls[6, 9]

Nano-bowls are polydisperse large spheres with one or more voids asymmetrically located which can even break at the surface of the aggregate. Given that the classification of the morphologies is made by inspection of 2D projections, the nano-bowls are present in different angles, it is often not clear if the void is indeed breaking the surface and, in the case that the void is facing the carbon side of the TEM grid, it is harder to differentiate it from a large compound micelles. For the purpose of this paper, we

consider a broken surface to the surface of nano-bowls with asymmetrically voids regardless if they break the surface or not. In most conditions, nano-bowls present only one asymmetric void, except for initial concentration of 0.1 mg/mL, addition rate of 1 mL/min and 40°C, were they present two or more.

Nano-bowls are ubiquitous throughout the state diagram and present different internal structures. At low concentration (0.1 mg/mL) the internal structures are either solid or with isolated pores while at higher concentration (1 and 10 mg/mL) the internal structures are hollow or present connected pores.

S(CP), P(CP): cubosomes and hexosomes[5]

The 2D projections of the internal structures with connected pores resemble bicontinuous structures. The precise classification of the structures into cubosomes or hexosomes requires further analysis by diffraction or electron tomography. For the purpose of this paper, we name all these different internal structures as internal structure with connected pores. These particles present either a solid or a porous surface (Figure S5).

P(H): Large compound vesicles[10]

Large compound vesicles are believed to be formed by the collapse and aggregation of vesicles. These structures have been observed during the formation of bicontinuous structures from vesicles.[11]

Size measurements

Particle size for each morphology present in each condition was obtained from TEM micrographs. When possible, at least 100 particles were measured for each condition.

In order to study the relationship between aggregate size, temperature and concentration, the size of all morphologies present was averaged for all water addition rate and plot against temperature as shown in Figure S12. Particle size increases with increasing temperature.

Coexistence of different morphologies

The presence of one single morphology per condition was encountered in 6 out of the 36 conditions (see Table S1). Under most conditions, at least two different morphologies coexist. We hypothesize that the coexistence of different morphologies under a certain condition is an indication of the morphologies being mechanistically related. We determine the predominant morphology by classifying an average of 100 particles per sample from the TEM micrographs.

S(S) and B(S) coexist in nine conditions at initial polymer concentration 0.1 mg/mL, (Table S1, Figure S8.a). Previous time-resolved TEM studies have been performed to unveil the formation mechanism of nano-bowls. [6, 9, 12] Aliquots taken during the self-assembly of polymers via the solvent switch method showed that first they form solid spheres, S(S).[6, 9, 12] Upon addition of water, the phase separation results in a polymer-rich phase and several solvent-rich bubbles, that eventually can coalesce into larger droplets. If such a droplet, usually asymmetrically located, is close to the edge of the sphere, the wall will break. Whether the droplets appear depends on how fast the solvent exchanges compared to the hardening of the shell of the large compound micelles, caused by the increase of the *T*g of the PS block. Liu *et al.* [9] observed for a random copolymer of P(S-$_{23}$MAA)-20K that the average diameter of B(S) is bigger than that of the S(S).

S(H) and S(CP) coexist in three conditions at initial polymer concentration of 1 mg/mL and in six conditions at initial polymer concentration of 10 mg/mL (Table S1, Figure S8.c). The mechanistic

connection between S(H) and S(CP) particles was showed by time-resolved TEM studies performed by different groups[13]. In Figure S8 the coexistence of S(H) and S(CP) (and P(H) and P(CP)) is shown for three different conditions. In Figure S10 a selection of morphologies suggest that these morphologies might be formed via fusion.

B(H) and B(CP) coexist in four conditions at initial polymer concentration 1 mg/mL and in 2 conditions at initial polymer concentration of 10 mg/mL (Table S1, Figure S9b, Figure S11). To the best of our knowledge, the B(CP) morphology has not been widely reported or investigated.

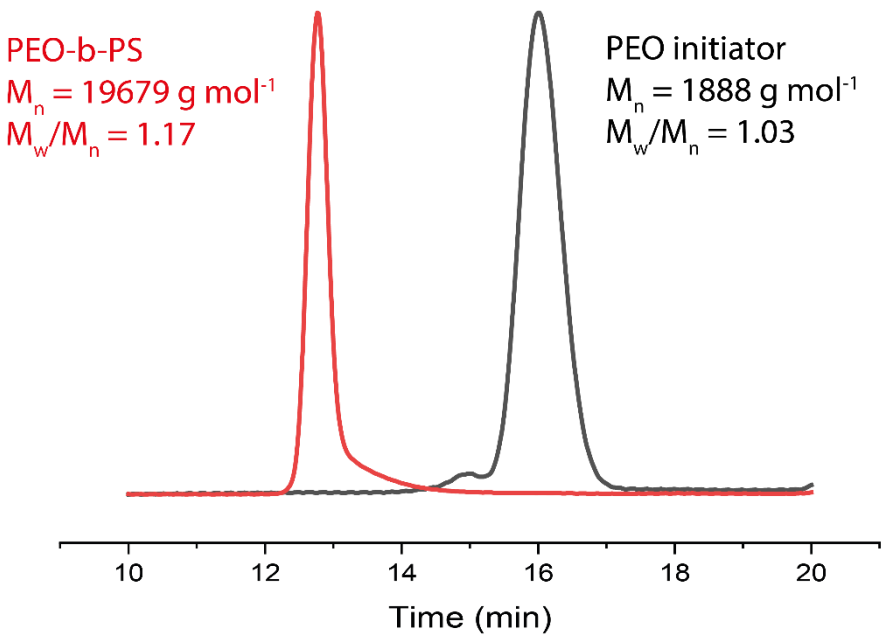

Figure S1. Characterization of PS_{250}-*b*-PEO_{45}. GPC curves obtained for PEO initiator and PS-*b*-PEO block copolymer. Two mixed bed columns (Mixed-C, Polymer Laboratories, 30 cm, 40 °C) were used and THF was selected as eluent. The system was calibrated using narrow molar mass polystyrene standards, ranging from 162 to 30230 Da.

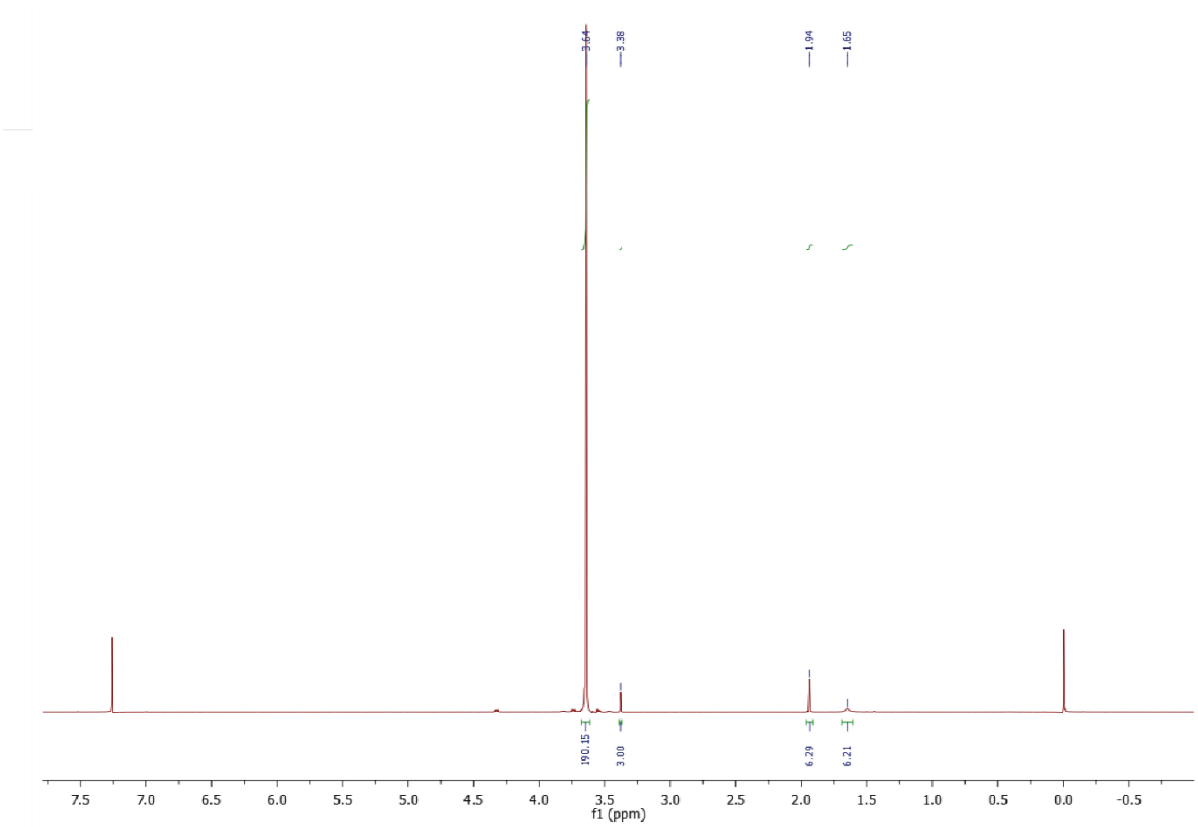

Figure S2 ^{1}H NMR (400 MHz) at 25 °C in $CDCl_3$ spectrum of PEO initiator used for the synthesis of PS_{250}-*b*-PEO_{45}.

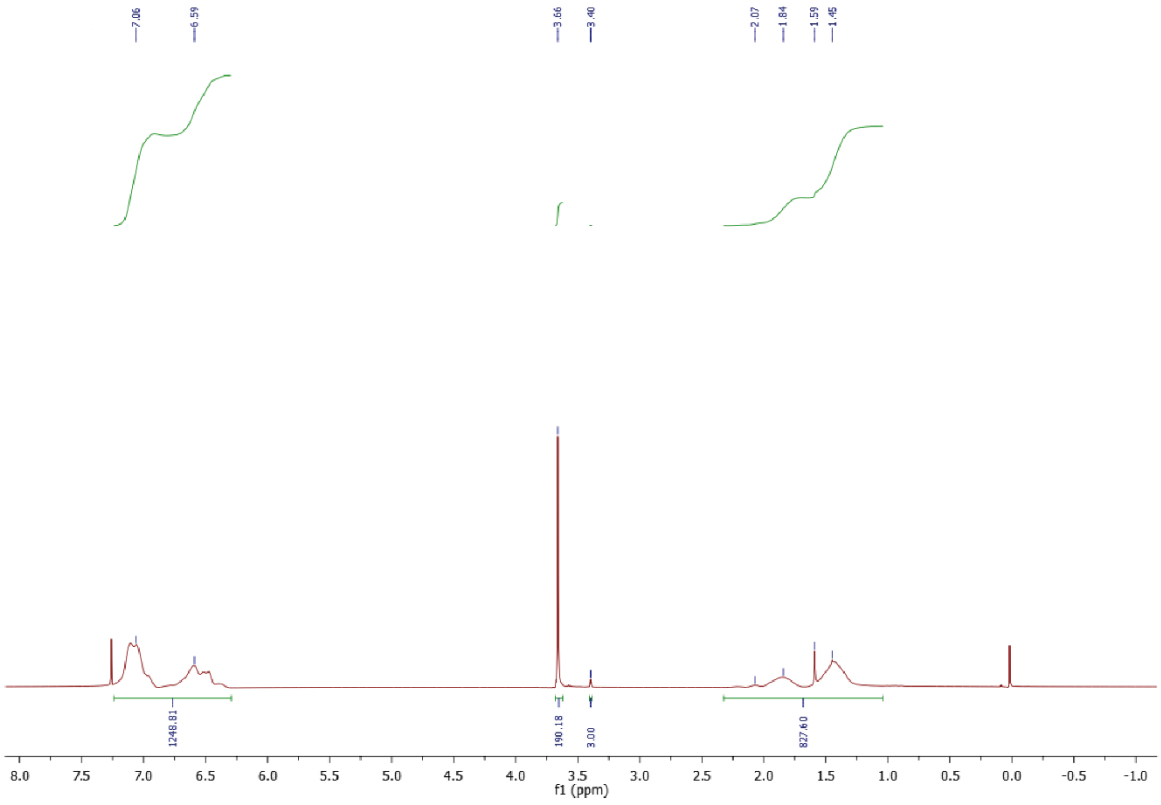

Figure S3 ^{1}H NMR (400 MHz) at 25 °C in $CDCl_3$ spectrum of PS_{250}-*b*-PEO_{45}.

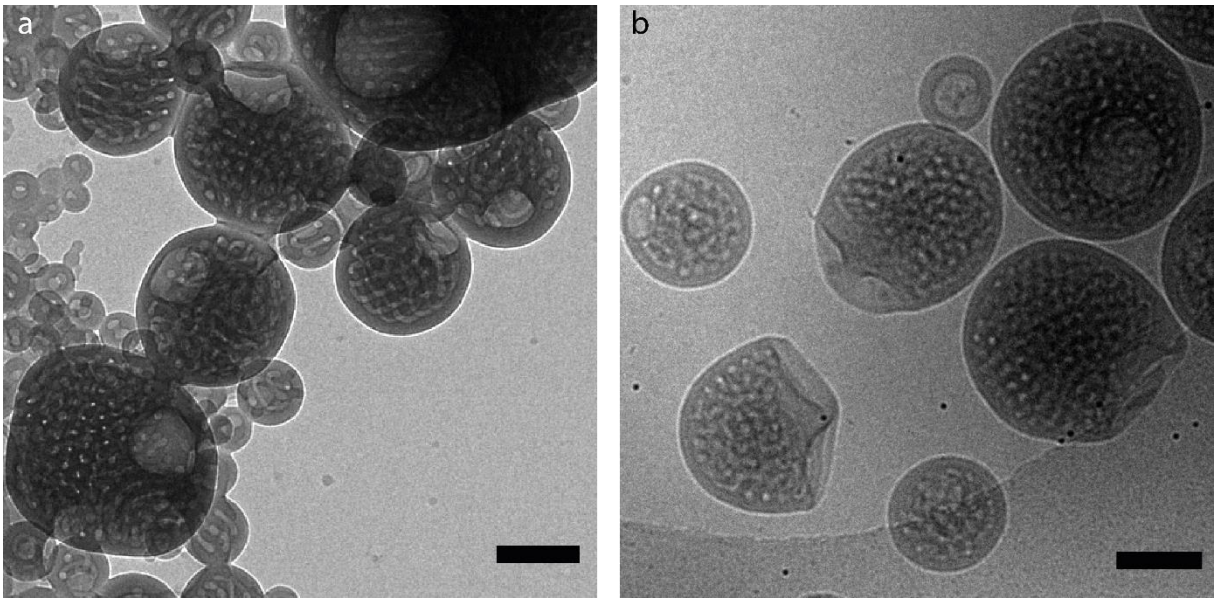

Figure S4: Comparison between dry state and cryo-TEM characterization of PS_{250}-*b*-PEO_{45} assembled at initial polymer concentration of 1 mg/mL, temperature 20 °C and rate addition 1 mL/h. a) dry state TEM and b) cryo TEM. Scale bars: 200 nm.

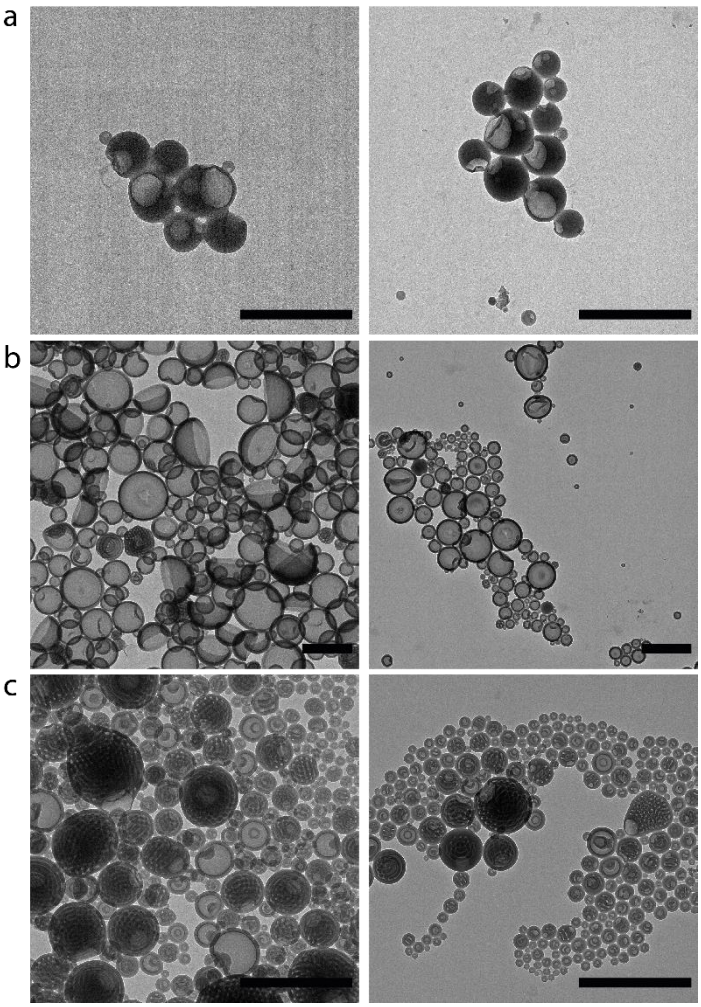

Figure S5: TEM characterization of assemblies performed with 1.5 years of difference. The samples were stored at room temperature. a) initial polymer concentration 0.01 mg/mL, temperature 4 °C and rate addition 1 mL/min, b) initial polymer concentration 10 mg/mL, temperature 40 °C and rate addition 1 mL/h and c) b) initial polymer concentration 10 mg/mL, temperature 40 °C and rate addition 1 mL/d. Scale bars: 1 µm.

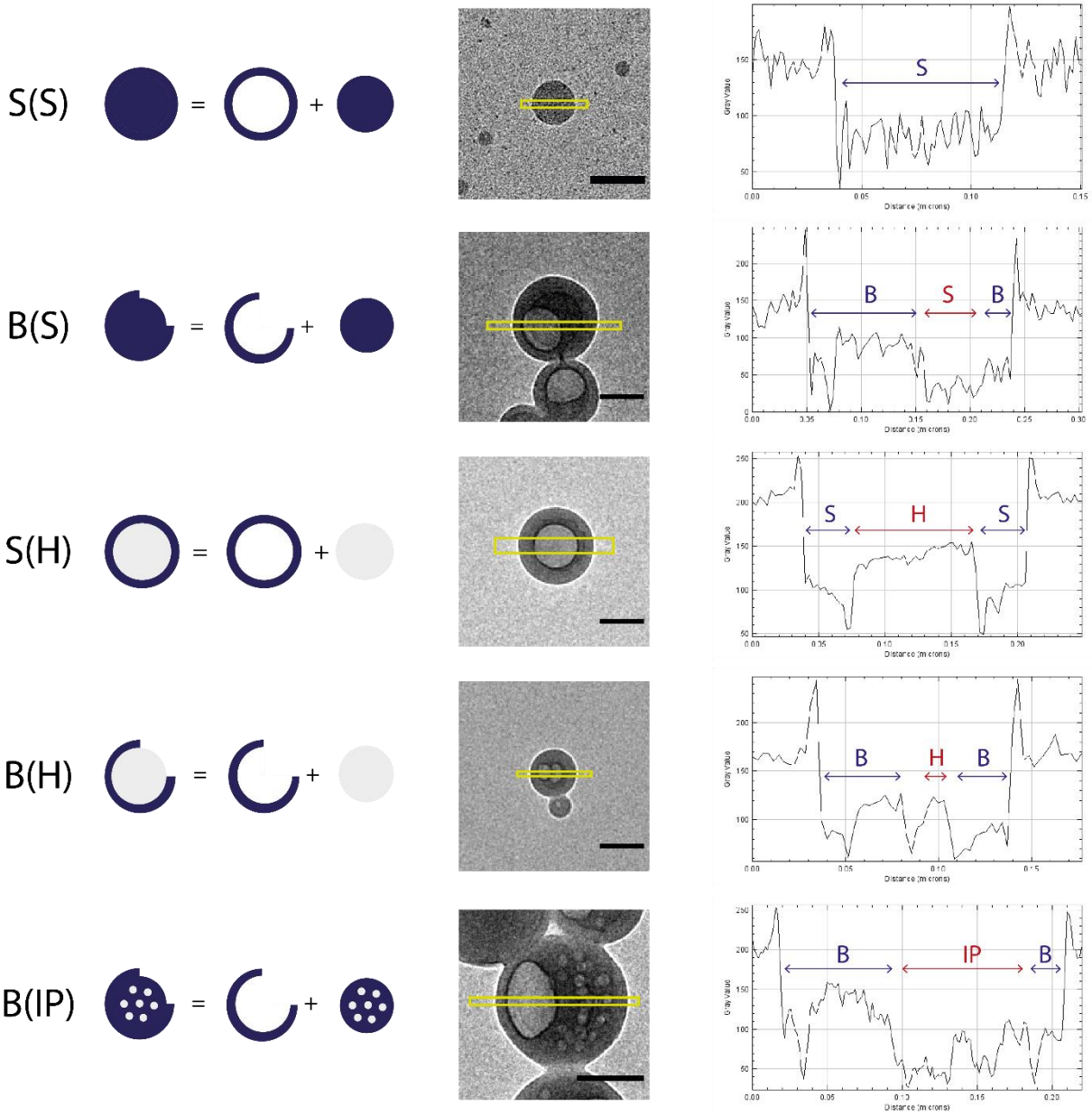
S(S)
=
+
S
B(S)
=
+
B
S
B
S(H)
=
+
S
H
S
B(H)
=
+
B
H
B
B(IP)
=
+
B
IP
B
Gray Value
Distance (microns)

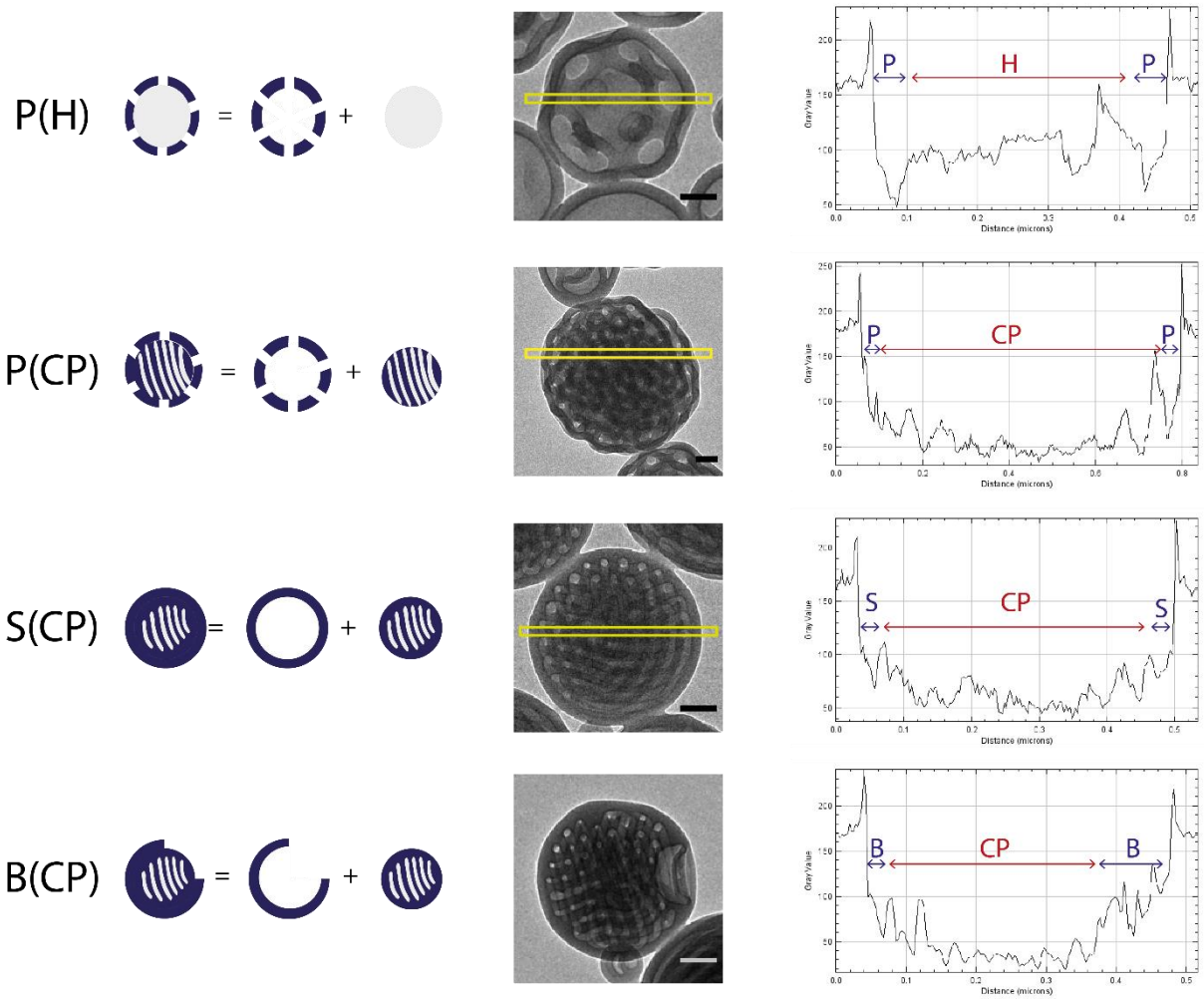

Figure S6: Classification of morphologies adopted by PS_{250}-*b*-PEO_{45}. The morphologies can be interpreted as a combination of a surface (solid **S**, broken B and porous **P**) and an internal structure (solid **S**, hollow **H**, with isolated pores **IP** and with connected pores **CP**). TEM micrographs (scale bars: 100 nm) are next to each scheme as an example of the morphology. A blue square shows the area from which an intensity profile was acquired. Careful inspection of the intensity profiles leads to the classification of the surface (in blue) and the internal structure (in red).

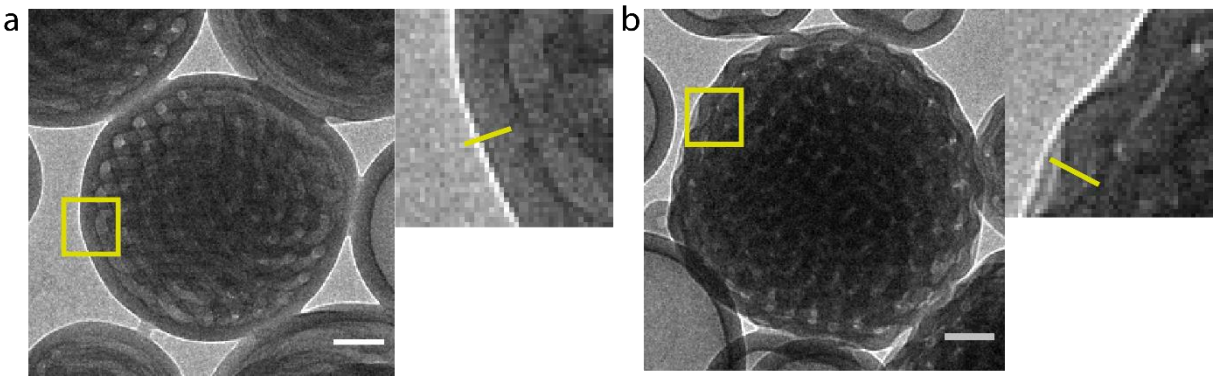

Figure S7: Difference between a solid surface and porous surface. a) S(CP) morphology and b) P(CP) morphology. The yellow squared is zoomed in. The overlap of membranes with different intensity in TEM indicates that the surface is porous (b) whereas the solid membrane observed in (a) indicates the surface in not porous. Scale bar: 100 nm.

State diagrams

Table S1. Morphologies overview for PS_{250}-*b*-PEO_{45}. In **bold** the most predominant morphology is shown, followed for the other morphologies in order of abundance. *: sample could not be characterized as no distinguishable aggregates were seen in TEM.

		4˚C	20˚C	40˚C	60˚C
0.1 mg/mL	1 mL/day	**S(S)**-B(S)	**S(S)**-B(S)-B(IP)	S(S)-B(S)	**S(S)**
	1 mL/hour	**B(S)**-S(S)	**S(S)**-B(S)	**S(S)**-B(S)	**B(S)**-B(IP)-S(S)
	1 mL/min	**B(IP)**-B(S)	**B(S)**-S(S)	**B(S)**	**B(S)**-S(S)
1 mg/mL	1 mL/day	**B(H)-**S(S)-B(IP)	**B(CP)-B(H)**	**S(H)-**S(CP)	**B(CP)**
	1 mL/hour	**B(H)-**S(S)	**B(H)**-**B(CP**)	**B(CP)-**B(H)	*
	1 mL/min	**S(H)-**S(CP)-B(CP)	**S(H)**-S(CP)	**B(CP)**	**B(CP)**
10 mg/mL	1 mL/day	**S(H)**-S(S)-S(CP)-S(CP)	**S(H)**-S(CP)	**B(H)-B(CP)**	**S(CP)**-S(H)
	1 mL/hour	**S(S)**-S(H)	**S(H)**	**S(H)**	**B(H)-B(CP)**-S(H)
	1 mL/min	**S(H)**-S(S)	**S(H)**-S(CP)-P(H)	**S(H)**-S(CP)-P(CP)	**S(CP)**-S(H)

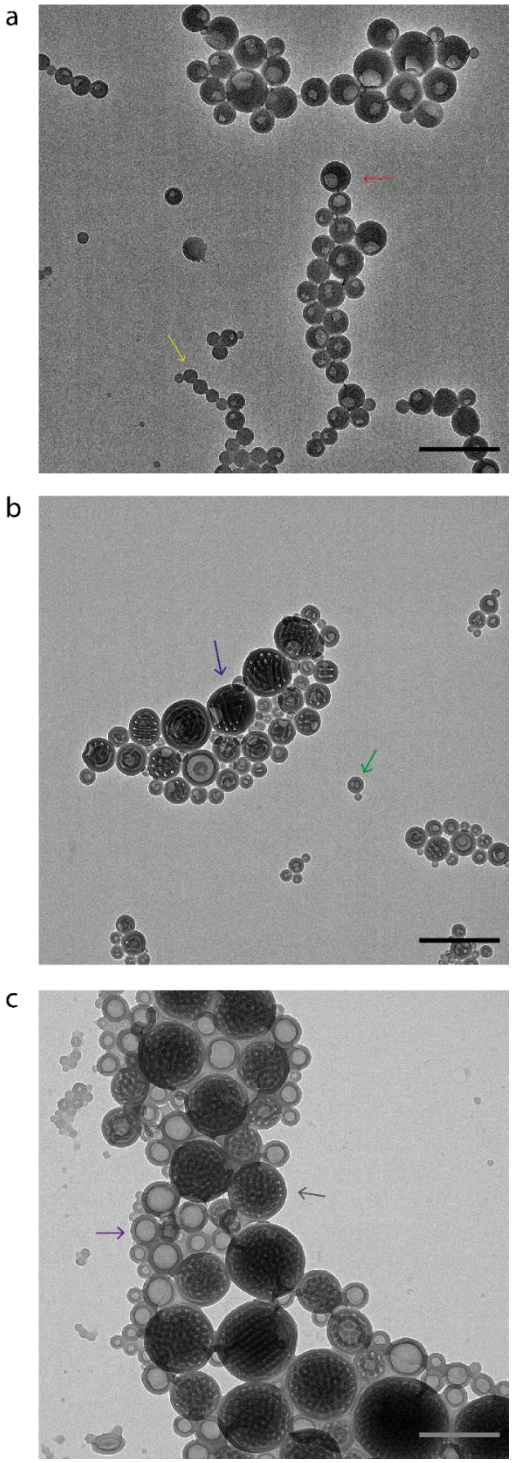

Figure S8: a) Coexistence of S(S) (yellow arrow) and B(S) (red arrow) for initial polymer concentration of 0.1 mg/mL, addition rate of 1 mL/min at 20 °C. b) Coexisting of B(H) (green arrow) and B(CP) (blue arrow) for initial polymer concentration of 10 mg/mL, addition rate 1 mL/d at 40 °C. c) Coexisting of S(H) (purple arrow) and B(CP) (gray arrow) for initial polymer concentration of 1 mg/mL, addition rate 1 mL/min at 20 °C. (Scale bar: 500 nm).

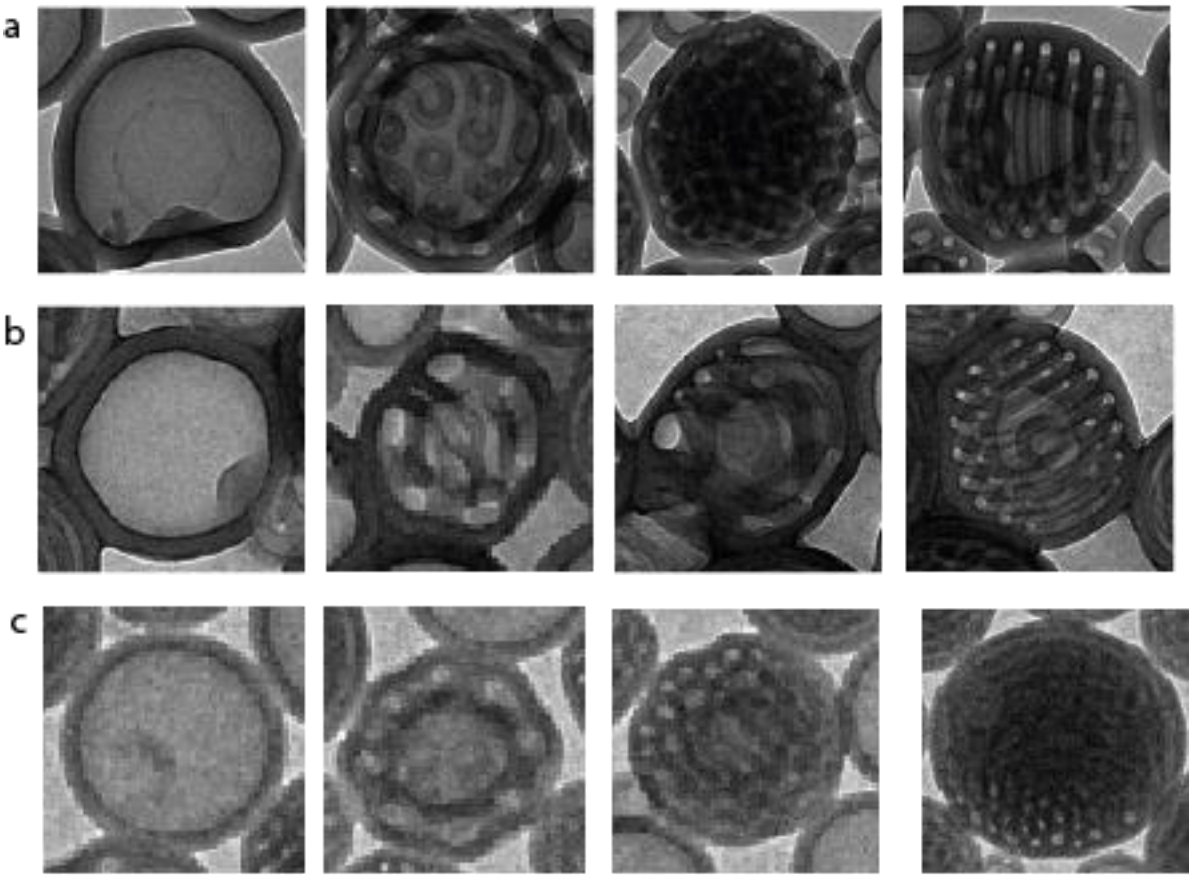

Figure S9. TEM characterization of the PS_{250}-*b*-PEO_{45} assemblies for initial polymer concentration 10 mg/mL at a) rate addition of 1 mL/min and 40 °C, b) rate addition of 1 mL/min and 60 °C and c) rate addition of 1 mL/h and 40 °C. The co-existence of S(H), P(H), P(CP) and S(CP) indicates that these morphologies are mechanistically related.

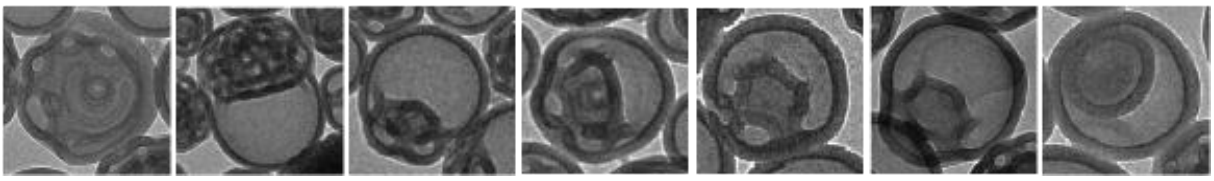

Figure S10. Kinetically trapped assemblies observed for PS_{250}-*b*-PEO_{45} assemblies at initial polymer concentration 10 mg/mL, 20 °C and rate addition of 1 mL/min. The selected images provide insight into a general morphology trend and show indication of fusion of particles to form aggregates with complex internal structure.

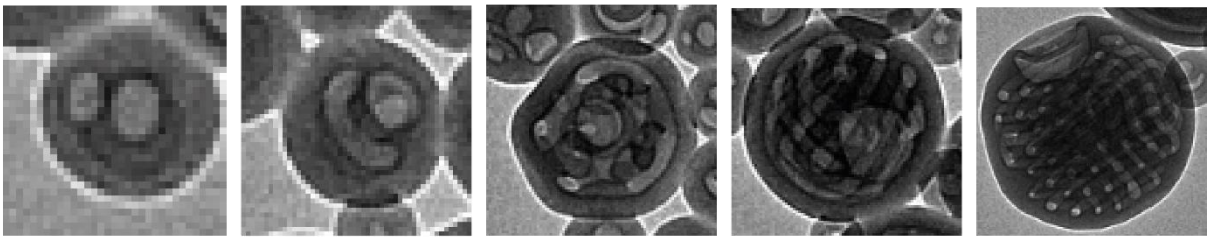

Figure S11. TEM characterization of the PS_{250}-*b*-PEO_{45} assemblies for initial polymer concentration 10 mg/mL, 40 °C and rate addition of 1 mL/h. B(H) and B(CP) morphologies coexist. The selected images show a general morphology trend in the formation of particles with broken surfaces and internal structure with connected pores but do not represent a temporal series.

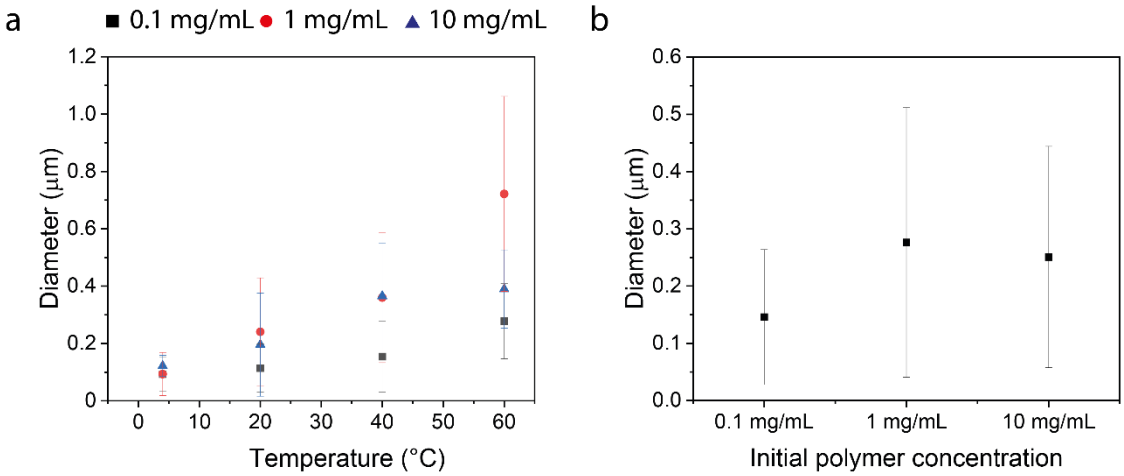

Figure S12: a) Average particle size for all morphologies by rate addition as a function of temperature and initial polymer concentration. b) Average particle size for all morphologies as a function of initial polymer concentration. The average particle size (without distinguishing between different morphologies) increases with temperature. A less pronounced increase in average size is observed with the increase of polymer concentration.

References

1. Q. Ying and B. Chu, *Macromolecules*, 1987, **20**, 362-366.
2. H. Friedrich, P. M. Frederik, G. de With and N. A. Sommerdijk, *Angew. Chem. Int. Ed.*, 2010, **49**, 7850-7858.
3. S. J. Holder and N. A. Sommerdijk, *Polym. Chem.*, 2011, **2**, 1018-1028.
4. A. L. Parry, P. H. Bomans, S. J. Holder, N. A. Sommerdijk and S. C. Biagini, *Angew. Chem.*, 2008, **47**, 8859-8862.
5. B. E. McKenzie, S. J. Holder and N. A. Sommerdijk, *Curr. Opin. Colloid Interface Sci.*, 2012, **17**, 343-349.
6. I. C. Riegel, A. Eisenberg, C. L. Petzhold and D. Samios, *Langmuir*, 2002, **18**, 3358-3363.
7. K. T. Kim, J. Zhu, S. A. Meeuwissen, J. J. L. M. Cornelissen, D. J. Pochan, R. J. Nolte and J. C. van Hest, *J. Am. Chem. Soc.*, 2010, **132**, 12522-12524.
8. T. Azzam and A. Eisenberg, *Langmuir*, 2010, **26**, 10513-10523.
9. X. Liu, J.-S. Kim, J. Wu and A. Eisenberg, *Macromolecules*, 2005, **38**, 6749-6751.
10. L. Zhang and A. Eisenberg, *Macromolecules*, 1996, **29**, 8805-8815.
11. Z. Lin, S. Liu, W. Mao, H. Tian, N. Wang, N. Zhang, F. Tian, L. Han, X. Feng and Y. Mai, *Angew. Chem.*, 2017, **56**, 7135-7140.
12. H. Sun, D. Liu and J. Du, *Chemical science*, 2019, **10**, 657-664.
13. C. K. Wong, X. Qiang, A. H. E. Müller and A. H. Gröschel, *Progress in Polymer Science*, 2020, **102**, 101211.